Equilibrium Compositions of Coexisting Garnet and Orthopyroxene: Experimental Determinations in the System FeO-MgO-Al2O3-SiO2, and Applications

Article *in* Journal of Petrology · February 1988

DOI: 10.1093/petrology/29.1.93 · Source: OAI

2 authors, including:

Jibamitra Ganguly
The University of Arizona
199 PUBLICATIONS **6,226** CITATIONS

SEE PROFILE

Equilibrium Compositions of Coexisting Garnet and Orthopyroxene: Experimental Determinations in the System $FeO–MgO–Al_2O_3–SiO_2$, and Applications

by HAN YEANG LEE* AND JIBAMITRA GANGULY

Department of Geosciences, University of Arizona Tucson, Arizona 85721

(Received 20 March 1987; revised typescript accepted 8 September 1987)

ABSTRACT

We have determined the Fe–Mg fractionation between coexisting garnet and orthopyroxene at 20–45 kb, 975–1400 °C, and the effect of iron on alumina solubility in orthopyroxene at 25 kb, 1200 °C, and 20 kb, 975 °C in the FMAS system. The equilibrium compositions were constrained by experiments with crystalline starting mixtures of garnet and orthopyroxene of known initial compositions in graphite capsules. All iron was assumed to be Fe^{2+}. A mixture of PbO with about 55 mol per cent PbF_2 proved very effective as a flux.

The experimental results do not suggest any significant dependence of K_D on Fe/Mg ratio at $T \gtrsim 1000$ °C. The $\ln K_D$ vs. $1/T$ data have been treated in terms of both linear and non-linear thermodynamic functional forms, and combined with the garnet mixing model of Ganguly & Saxena (1984) to develop geothermometric expressions relating temperature to K_D and Ca and Mn concentrations in garnet.

The effect of Fe is similar to that of Ca and Cr^{3+} in reducing the alumina solubility in orthopyroxene in equilibrium with garnet relative to that in the MAS system. Thus, the direct application of the alumina solubility data in the MAS system to natural assemblages could lead to significant overestimation of pressure, probably by about 5 kb for the relatively common garnet-lherzolites with about 25 mol per cent $Ca+Fe^{2+}$ in garnet and about 1 wt. per cent Al_2O_3 in orthopyroxene.

INTRODUCTION

The equilibrium compositions of coexisting garnet and orthopyroxene have been widely recognized as potential indicators of the P–T condition of formation of a variety of natural assemblages, especially those formed at granulite facies metamorphic conditions and in the earth's upper mantle. The primary objective of the present work has been to determine the equilibrium fractionation of Fe and Mg between the two minerals as a function of temperature and Fe/Mg ratio in the system $FeO–MgO–Al_2O_3–SiO_2$(FMAS), and to apply these data to formulate an exchange geothermometer, which should be applicable to a wide variety of natural garnet-orthopyroxene assemblages. Limited experimental work has also been carried out to constrain the effect of Fe/Mg ratio on the Al_2O_3 solubility in orthopyroxene in equilibrium with garnet, which constitutes the most extensively used geobarometer for mantle derived rocks.

Previous experimental and theoretical studies of the compositional properties of coexisting garnet and orthopyroxene include Akella & Boyd (1973), Hensen (1973), Wood (1974), Harley & Green (1982), Kawasaki & Matsui (1983), Harley (1984) and Sen & Bhattacharya (1984). However, little work has been done so far to experimentally constrain the equi-

*Present address: Korea Institute of Energy and Resources, 219–5 Garibong-Dong, Guru-Gu, Seoul, Korea.

librium compositions of coexisting garnet and orthopyroxene by determining compositional changes in crystalline starting materials, which is the most unambigous way of determining equilibrium compositions at a given P, T, X condition.

EXPERIMENTAL METHODS

Apparatus, sample configurations and P–T *measurements*

All experiments were carried out in an end-loaded Piston-Cylinder apparatus, using 1/2, 3/4 or 1 in. carbide-core pressure vessels and carbide pistons. NaCl or CsCl were used as sleeves around graphite furnaces in the pressure cell (Fig. 1) in the manner suggested by Boettcher *et al.* (1981), which greatly reduced the distortion of the furnace due to differential compression of pressure cell materials. No friction correction was made to the nominal pressure as salt sleeves offer very little frictional resistance to pressure (Mirwald *et al.*, 1975). CsCl has a much lower thermal conductivity than NaCl, and thus helps reduce fracturing of the carbide cores due to thermal stress in relatively high P–T runs (Elphick *et al.*, 1985).

The pressure cells were wrapped with 0·002 in. thick lead foil, and the inner wall of the

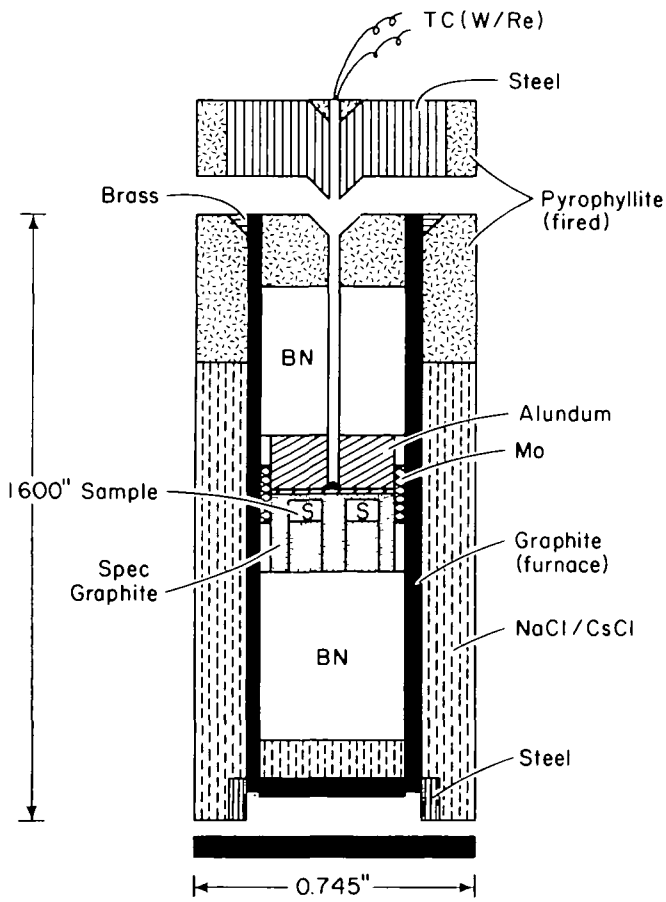

FIG 1. Schematic illustration of the cross section of a typical pressure cell used in the experiments in Piston-Cylinder apparatus.

pressure core was coated with hydrogen free 'Molykote' (MoS_2) lubricant to reduce friction at high pressures. All pressure cells were dried in an oven at least for 12 h at ~150 °C before loading inside a pressure vessel. Samples were packed inside spectrographic quality graphite disks—each hole being tightly fitted with a graphite lid.

Temperatures were measured with W3 per cent Re–W25 per cent Re thermocouples and encased in 99·99 per cent Al_2O_3 ceramic tubings. The W–Re thermocouple is known to have superior mechanical and chemical stability, compared to Chromel-alumel and Pt–Rh thermocouples. To minimize thermocouple 'poisoning' by reaction with pressure cell material, a 0·015–0·020 in. alundum (99·9 per cent Al_2O_3) disk was placed between the thermocouple junction and the top surface of the graphite container. The thermocouple junction was ~0·050 in. from the sample. The thickness of the sample disk within a graphite container was within 0·12 in. Following Elphick *et al.* (1985) the graphite container was surrounded by a 0·20 in. high Mo ring, which was shorted to the furnace. The central sections of the furnace and Mo ring coincided with the top surface of the sample disk. This configuration reduced the temperature difference between the thermocouple junction and the lower surface of the sample disk to within 5 °C (Elphick *et al.*, 1985). The nominal temperatures were corrected for the pressure effect on the e.m.f. of W/Re thermocouple according to the method discussed by Lane & Ganguly (1980). The corrected temperatures are 6–9 °C higher than the nominal ones. From our earlier experience with the problem of thermocouple stability in this type of pressure cell (e.g., Elphick *et al.*, 1985), we believe that the true sample temperature for any run above 1200 °C was within ±10 °C of that reported for the run. The accuracy of temperature measurement is better at lower temperatures.

Analytical methods

The run products were analyzed with an automated ARL scanning electron microprobe using a 15 kV accelerating voltage and a 25 nA sample current. The X-ray intensity and background for each measurement was corrected automatically by the computer program Task II (McCarthy, 1975) and the analytical data were reduced by the Bence–Albee method (Bence & Albee, 1968). Instrumental drift was handled by recalibrating at approximately 3-h intervals. The standards used were as follows: Anorthite for Al and Ca, diopside for Mg and Si, fayalite for Fe, rhodonite for Mn, albite for Na, chromite for Cr, sphene for Ti, and orthoclase for K.

Only those analyses which had total wt. per cent oxide between 99 and 101, and satisfied the theoretical stoichiometry of the mineral within 2 per cent, were considered acceptable for the determination of K_D. All iron was assumed to be in the ferrous state. (Calculations of f_{O_2} condition in the C–O_2 system in the presence of graphite suggests that f_{O_2} values at the run conditions were between those defined by QFM and WI buffers, and within ±2 log units of the WM buffer. The f_{O_2} for the C–H_2O + graphite system lies between those of C–O_2 + graphite system and the WI buffer.)

Starting materials

Natural and synthetic garnet and orthopyroxene were used to prepare starting materials for studying the equilibrium compositions of coexisting garnet and orthopyroxene. Natural samples with $X_{Fe} + X_{Mg} = 0{\cdot}97$ were separated from various rocks and handpicked under binocular microscope. The compositions of starting materials are given in Table 1.

TABLE 1

Microprobe analysis of starting materials

	Orthopyroxenes					*Garnet*		
	Opx/1	*Opx/2*	*Opx/3*	*Opx/4*	*Opx/5*	*Gt/1*	*Gt/2*	*Gt/3*
FeO*	9·32	46·76	31·14	—	34·86	35·37	22·74	0·04
MgO	33·81	5·09	17·80	37·77	13·55	5·34	13·01	29·80
SiO_2	56·30	47·57	51 79	56·62	50·28	38·48	39·18	44·95
Al_2O_3	0·08	0·75	0·07	6·43	0·03	21·33	23·25	25·74
CaO	0·32	0·61	—	—	0·58	0·40	1·80	0·19
MnO	0·05	0·05	—	—	1·30	0·03	0·49	—
Cr_2O_3	—	0·01	—	—	—	—	—	—
TiO_2	—	0·02	—	—	—	0·02	—	—
Na_2O	—	0·03	—	—	—	0·05	0·02	—
NiO	0·05	—	—	—	0·07	—	—	—
K_2O	—	—	—	—	—	—	—	—
Total	99 94	100·90	100·70	100·82	100·68	101·09	100·40	100·72
Fe	0·545	3·260	1·999	—	2 306	2·322	1·424	0·002
Mg	3·529	0·635	2·037	3·734	1 597	0·624	1·452	2·960
Si	3·942	3·966	3·976	3·755	3·975	3·021	2 934	2·994
Al	0·006	0·074	0·006	0·502	0·002	1·973	2·051	2·020
Ca	0·023	0·054	—	—	0·049	0·040	0·144	0·013
Mn	0·003	0·003	—	—	0·086	0·001	0·031	—
Cr	—	—	—	—	—	—	—	—
Ti	—	—	—	—	—	0·001	—	—
Na	—	0·004	—	—	—	0·007	0·003	—
Ni	0·002	—	—	—	—	—	—	—
K	—	—	—	—	—	—	—	—
Cation total O:12	8·050	7·996	8·018	8·091	8·015	7·989	8·039	7·989
Fe/Mg	0·154	5 154	0·981	0·000	1·443	3·717	0·980	0·000
Fe/(Fe+Mg)	0·133	0·837	0·495	0·000	0·590	0·788	0·495	0·000

Opx/1: Sample from Telmark, Norway (UCLA Mineral Museum)
Opx/2: Sample No. XYZ, Ramberg & Devore (1951)
Opx/3: Synthetic sample
Opx/4: Synthetic sample
Opx/5: Sample No. 5, Butler
Gt/1: Natural sample, Schneider Co.
Gt/2: Natural sample No. 143895, Smithsonian Collection
Gt/3: Synthetic pyrope
* All iron assumed to be FeO

Pyrope

Pyrope was synthesized hydrothermally in a sealed gold capsule from a stoichiometric mixture of reagent grade MgO, SiO_2, and Al_2O_3 at 25 kb, 1000°C for 24 h. The X-ray diffraction pattern showed single phase pyrope.

Non-aluminous orthopyroxene

Non-alyminous orthopyroxene was synthesized from a mixture of reagent grade MgO, Fe_2O_3, and SiO_2 under dry conditions in a graphite capsule at 25 kb, 1200°C for 48 h. The run product consisted of grains 200 μm or larger. The Fe/(Fe+Mg) ratio varied between 0·47 and 0·50, considering the variations between grain to grain and compositional zoning within individual grains. The average Fe/(Fe+Mg) ratio of the run product was 0·49 compared to the intended ratio of 0·6 of the starting material. Alloying of Fe with the

graphite capsule (and weighing error) might have been responsible for the lower concentration of Fe in the run product. However, the X-ray diffraction pattern showed single phase orthopyroxene.

Aluminous orthopyroxene

Aluminous orthopyroxene was synthesized hydrothermally in a sealed gold capsule from a mixture of reagent grade MgO, Al_2O_3, and SiO_2 at 20 kb, 1100 °C for 48 h. The mixture was seeded with 5 wt. per cent of synthetic aluminous enstatite (12 wt. per cent Al_2O_3) which was synthesized from an oxide mixture with 5 wt. per cent of natural pyroxene, OPx/1 (Table 1). The run product showed broad X-ray reflections implying significant inhomogeneity in the concentration of Al_2O_3. To improve homogeneity, the run product was crushed and recycled at 25 kb, 1350 °C, for 48 h in a dry graphite container. The X-ray peaks of the recycled product were sharper, and microprobe analyses of several grains yielded an average Al_2O_3 content of 6·5 wt. per cent with a range of 5–9 wt. per cent.

Two types of starting mixtures were prepared from the natural and synthetic minerals for the determination of equilibrium Fe–Mg fractionation between garnet and orthpyroxene such that the equilibrium K_D value could be approached from both higher and lower initial values during an experiment. Along with the Fe/Mg ratio, the Al_2O_3 content of the orthopyroxene also evolved toward equilibrium value in an experiment consisting of a mixture of orthopyroxene and garnet (see later for a thermodynamic analysis of the effect of Al_2O_3 on K_D). The starting orthopyroxene was mostly non-aluminous. Limited experiments were performed to approach the equilibrium alumina solubility from a supersaturated composition, using a mixture of the synthetic aluminous enstatite and garnet.

Flux material

A number of workers (e.g., Gasparik, 1983; Gasparik & Newton, 1984) have successfully used PbO flux to catalyze cation exchange reactions between silicates. However, because of its relatively high melting temperature, the use of PbO as a flux material had to be essentially limited above 1200 °C in high P–T experimental studies. In this work, we have used a mixture of PbO and PbF_2 as flux material. Unfortunately, there are no data on the melting behavior of this mixture under high pressure. The 1 b binary phase diagram (Sandonini, 1914, quoted in Levin *et al.*, 1964) shows the eutectic point for the system at about 490 °C (compared to 888 °C for the melting of pure PbO). The results of a trial run with two flux compositions (0·75 PbF_2 and 0·55 PbF_2) loaded separately with Gt–OPx mixtures within a graphite disk suggested 0·55 PbF_2 + 0·45 PbO to be a relatively effective flux composition at the high P–T conditions of these experiments.

The effectiveness of PbO–PbF_2 flux in promoting Fe–Mg exchange between garnet and orthopyroxene is clearly demonstrated by a run at 30 kb, 1200 °C for 2 days. A small portion of a Gt–OPx mixture was mixed with the flux and packed inside one of the sample holes of a two-hole graphite disk, the other hole containing a portion of the same mixture, but without the flux. As illustrated in Fig. 2, the products of the fluxed run showed a significantly larger shift of composition toward equilibrium.

The PbO–PbF_2 flux was found to melt substantially in the lowest temperature experiment, 750 °C at 20 kb, attempted in this work. However, we failed to get an adequate exchange reaction below 975 °C. Part of the flux was usually converted to Pb by reaction with graphite capsule. As Pb has a relatively lower melting temperature (Akella *et al.*, 1973), the reduction of PbO to Pb should promote melting of the flux. The flux dissolved a substantial portion of the initial sample (~40–60 per cent), and the residual material sank

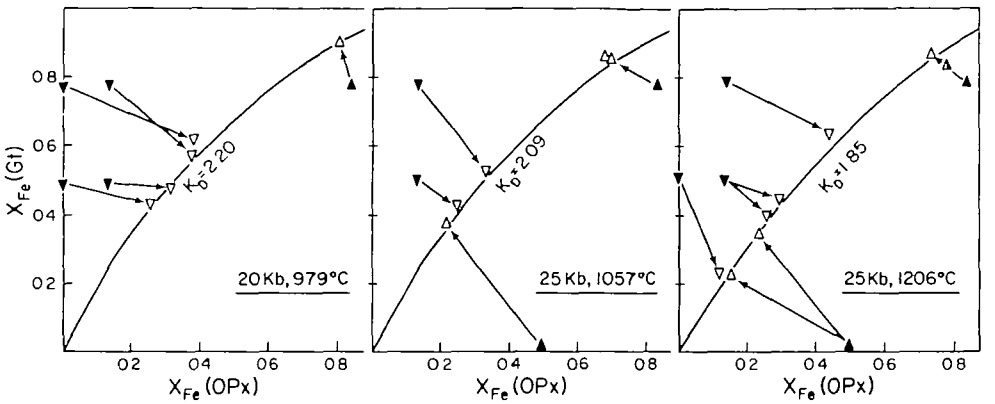

FIG. 2 Fractionation of Fe and Mg between coexisting garnet and orthopyroxene at selected P–T conditions, X_{Fe} = Fe/(Fe+Mg). All Fe is assumed to be divalent. Solid triangles starting composition; half-filled and open triangles: final compositions in dry run and in runs made with PbO–PbF_2 flux, respectively; arrows: direction of evolution of compositions. The development of two different final compositions from the same starting composition at 25 kb, 1206 °C is a consequence of different Gt/OPx ratios. All runs were in graphite capsules.

to the bottom of the graphite container. Microprobe analyses of the glassy material near the top of the container showed Pb, F, Fe, Mg, Ca, Al, Si, Cs, and Cl, the last two elements being derived from the insulating CsCl sleeve around graphite furnace of the pressure cell. The substitution of Pb and F within the silicates in all run products was found to be limited to 0·1–0·3 wt. per cent, which is too dilute to have any significant effect on the equilibrium compositions of coexisting garnet and orthopyroxene.

Owing to the dissolution of the sample in the flux, the choice of the optimal flux to sample ratio that would promote adequate reaction, but at the same time retain enough undissolved sample for microprobe analysis, appeared to be a tricky problem. In several runs, the entire samples were dissolved in the flux. The flux to sample ratio in the successful runs are shown in Table 2.

EXPERIMENTAL RESULTS AND THERMODYNAMIC ANALYSIS

Fe-Mg fractionation between garnet and orthopyroxene

The run data are summarized in Table 2, and the compositions of coexisting garnet and orthopyroxene at *selected* P–T conditions are illustrated in Fig. 2. Figure 3 shows the final K_D vs. X_{Fe}^{Gt} at each P–T condition investigated in this work. Both garnet and orthopyroxene usually displayed significant compositional inhomogeneities. Consequently, equilibrium compositions of coexisting garnet and orthopyroxene were determined on the basis of microprobe analyses made as close to their mutual contacts as possible, but without introducing 'edge' effects (Elphick, *et al.*, 1985; Ganguly, *et al.*, 1988).

The Fe^{2+}–Mg fractionation between garnet and orthopyroxene can be treated in terms of the following exchange equilibrium

$$\underset{\text{Gt}}{1/3\ Mg_3Al_2Si_3O_{12}} + \underset{\text{OPx}}{FeSiO_3} \rightleftarrows \underset{\text{Gt}}{1/3\ Fe_3Al_2Si_3O_{12}} + \underset{\text{OPx}}{MgSiO_3}. \qquad \text{(a)}$$

TABLE 2

Summary of selected run data

*Nominal** T°C	P, *kb*	*Time h*	*Starting mixture*	*Flux/sample wt. ratio*	*Initial* K_D	*Initial Al_2O_3 wt. per cent in OPx*	X_{Fe}^{Gt}	X_{Fe}^{OPx}	*Results† Al_2O_3 wt per cent in OPx*	*Final* K_D
975±5	20±0·5	168	Opx/4, Gt/2	0·80	∞	6·4	0·44	0·26	3·75	2.17
			Opx/1, Gt/2	0·80	6·36	0·08	0·49	0·31	2·85	2·14
			Opx/1, Gt/1	0·80	2·41	0·08	0·56	0·37	2·55	2·21
			Opx/4, Gt/1	0·80	∞	6·43	0·58	0·38	2·18	2·24
			Opx/2, Gt/1	0·80	0·72	0·75	0·91	0·83	1·44	2·23
1050±5	26±1	168	Opx/3, Gt/3	0·80	0·00	0·07	0·36	0·21	2·75	2·12
			Opx/1, Gt/2	0·80	6·36	0·08	0·42	0·27	2·44	1·97
			Opx/1, Gt/1	0·80	2·41	0·08	0·53	0·34	2·31	2·15
			Opx/2, Gt/1	0·80	0·72	0·75	0·85	0·72	0·76	2 11
1100±10	25±0·5	61	Opx/1, Gt/1	0·10	2·41	0·08	0·55	0·37	0·72	2·06
			Opx/2, Gt/1	0·10	0·72	0·75	0·79	0·65	1·19	2·02
1200±5	26±1	120	Opx/4, Gt/2	0·10	∞	6·43	0·22	0·13	3·90	1.83
			Opx/1, Gt/2	0·10	6·36	0·08	0·44	0·30	2·91	1·80
			Opx/1, Gt/2	0·10	6·36	0·08	0·40	0·25	3·18	1·96
			Opx/3, Gt/3	0·10	0·00	0·07	0·34	0·22	3·64	1·89
			Opx/3, Gt/3	0·10	0·00	0·07	0·24	0·15	4·23	1 77
1200±10	25·5±0·5	55	Opx/1, Gt/2	0·05	2·41	0·08	0·64	0·47	2·61	1·98
1200±10	32·5±1·5	48	Opx/2, Gt/1	0·05	0·72	0·75	0·84	0·74	1·46	1·83
1300±10	37.5±0·5	24	Opx/1, Gt/1	0·05	2.41	0·08	0·46	0·32	3.14	1·76
1300±5	39·5±0·5	48	Opx/2, Gt/1	0·00	0·72	0·75	0·81	0·70	1·79	1·80
1400±5	45·5±0·5	24	Opx/1, Gt/1	0·00	2.41	0·08	0·55	0·43	2·31	1·60
1400±5	43·5±0·5	45	Opx/2, Gt/2	0·00	0·19	0·75	0·61	0·48	2 23	1·64
1400±5	43·3±0·5	45	Opx/5, Gt/2	0·00	0·68	0·03	0·63	0·51	2·15	1·60

* The temperatures should be revised upward, as follows, to correct for the pressure effect on the e.m.f. of W–Re thermocouple: 975 to 979, 1050 to 1057, 1100 to 1104, 1200 to 1206, 1300 to 1305, 1400 to 1407.

†Average of at least 20 spot analyses.

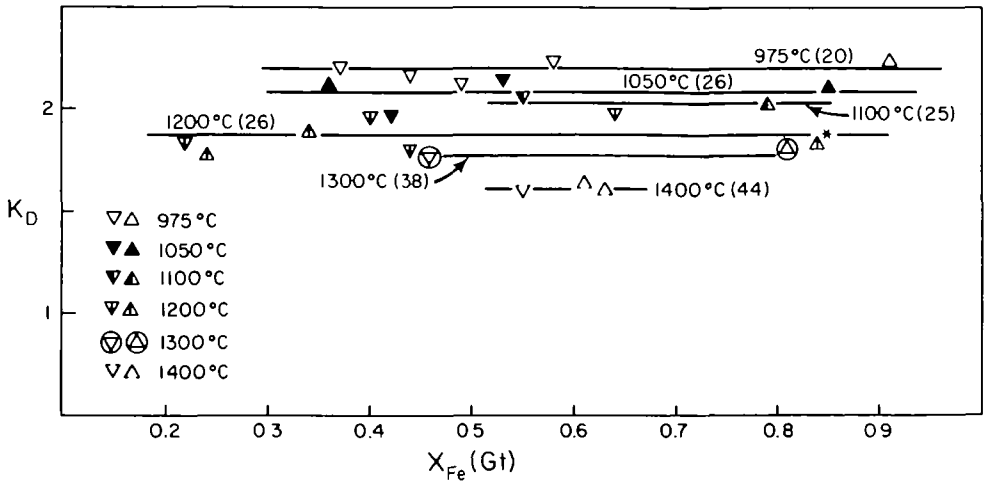

FIG. 3. K_D vs X_{Fe} (Gt) determined at various P–T conditions. The numbers within parentheses are nominal pressure in kb; the temperatures are nominal values (see Table 2 for correction). The symbols point toward the direction of approach of equilibrium. The 1200°C run marked by asterisk is at 32·5 kb; at 26 kb, the K_D value should be reduced by 0·1 (see text).

Thus, at equilibrium

$$K_{(a)} = \left[\frac{X_{Fe}^{Gt} X_{Mg}^{OPx}}{X_{Mg}^{Gt} X_{Fe}^{OPx}}\right] \left[\frac{\gamma_{Fe}^{Gt} \gamma_{Mg}^{OPx}}{\gamma_{Mg}^{Gt} \gamma_{Fe}^{OPx}}\right]$$

$$= \left[\frac{(Fe/Mg)^{Gt}}{(Fe/Mg)^{OPx}}\right] \left[\frac{(\gamma_{Fe}/\gamma_{Mg})^{Gt}}{(\gamma_{Fe}/\gamma_{Mg})^{OPx}}\right] \quad (1)$$

where $K_{(a)}$ is the equilibrium constant of reaction (a), and γ is the activity coefficient of the specified end-member component on a one-cation basis. We define the quantities within the first and second square brackets as K_D (distribution coefficient) and K_γ, respectively.

The data presented in Figs. 2 and 3 suggest the K_D to be essentially independent of Fe/Mg ratio at $T \gtrsim 1000$°C.This conclusion is corroborated by the extensive data of Kawasaki & Matsui (1983, Fig. 4) at 1100 and 1300°C. The simplest explanation for this lack of compositional dependence of K_D is that Fe and Mg mix essentially ideally in both garnet and orthopyroxene at $T \gtrsim 1000$°C. Alternatively, it is possible, as discussed further in the next section, that the nonideal Fe–Mg interactions in the two minerals effectively compensate for one another at these temperatures. At any rate, since $K_\gamma \simeq$ constant at $T \gtrsim 1000$°C, the corresponding derivative properties of K_D and K are essentially the same at the experimental conditions. We can, thus, reduce the polybaric Fe–Mg fractionation data to an arbitrary isobaric condition of 25 kb as follows.

$$\left(\frac{\partial \ln K_D}{\partial P}\right)_T \approx \left(\frac{\partial \ln K}{\partial P}\right)_T = -\frac{\Delta V^\circ}{RT} \quad (2.1)$$

or

$$\ln K_D(25\text{kb}, T) \approx \ln K_D(P, T) - \int_P^{25} \frac{\Delta V^\circ}{RT}\, dP. \quad (2.2)$$

Since the end-member components of a solid solution have similar pressure dependences,

it is a common practice to assume ΔV° of an exchange equilibrium to be effectively independent of pressure, at least over a few tens of kilobars. The molar volumes for the pure end members are taken from the measurements on synthetic samples by Charlu *et al.* (1975) and Chatillon-Colinet *et al.* (1983a, b). These data yield ΔV° (1 b, 298 K) $= -0{\cdot}977$ cm^3. (The slightly different V° values for pyrope and almandine reported by Kawasaki & Matsui (1977) do not materially affect ΔV°.) As compared to this, we find, using the compressibility data compiled by Chatterjee (1987), ΔV° (10 kb, 298 K) $= -0{\cdot}977$ cm^3 and ΔV° (50 kb, 298 K) $= -0{\cdot}975$ cm^3. The effect of thermal expansion on ΔV° is likewise expected to be very small. Thus, we have integrated the last term in eqn. (2.2) assuming ΔV° to be independent of pressure in the range of pressures of these experiments (20–45 kb), and using the 1 b, 298 K value. This procedure introduces negligible error in the calculation of $\ln K_D$ as a function of temperature under isobaric condition.

Linear least squared regression of the reduced isobaric $\ln K_D$ data vs. $1/T$ yields the following relation ($r = 0{\cdot}96$)

$$\ln K_D(25\text{kb}) = \frac{2269(\pm 142)}{T(\text{K})} - 0{\cdot}96 \tag{3.1}$$

or, using (2.2),

$$\ln K_D = \frac{1971(\pm 142) + 11{\cdot}9\,P(\text{kb})}{T(\text{K})} - 0{\cdot}96 \tag{3.2}$$

where the uncertainties represent one σ values. All K_D values from Table 2 have been used for the regression. Expression (3.2) yields a value of ΔH°_a of -3916 (± 282) cal at 1 b, 975–1400 °C. An error of 10 per cent in the ΔV^0 term changes the coefficient of $1/T$ by ~ 25, which is negligible compared to the magnitude of this coefficient.

The linear fit of $\ln K_D$ vs. $1/T$ implies that the ΔC^0_p of the exchange equilibrium, a, is zero. However, the experimental data also permit a nonlinear fit, and there is no *a priori* reason for assuming ΔC°_p to be zero. A simple nonlinear form of $\ln K$ vs. $1/T$ can be derived, as follows, assuming a constant but nonzero value of ΔC°_p. Thus, setting $\Delta C^\circ_p = a \neq 0$, we have $\Delta H^\circ = \Delta H_1 + a\ T$ and $\Delta S^\circ = \Delta S_1 + a\ \ln T$, where ΔH_1 and ΔS_1 are constants of integration. Consequently,

$$\begin{aligned} \ln K &= -(\Delta H^\circ - T\Delta S^\circ)/RT \\ &= A + B/T + C \ln T \end{aligned} \tag{4}$$

where $A = (\Delta S_1 - a)/R$, $B = -\Delta H_1/R$, and $C = a/R = \Delta C^\circ_p/R$. Using the thermodynamic relation $\partial \ln K/\partial(1/T) = -\Delta H^\circ/R$, we have from (4) $\Delta H^\circ_a = (CT - B)\,R$.

Stepwise regression of the $\ln K_D$, normalized to 25 kb, vs. $1/T$ and $\ln T$ shows that the variable $1/T$ is statistically redundant. We, thus, obtain the following fit to the experimental data ($r = 0{\cdot}97$).

$$\ln K_D(25\text{kb}) = 12{\cdot}067 - 1{\cdot}574 \ln T \tag{5.1}$$

or using (2.2),

$$\ln K_D = 12{\cdot}067 - 1{\cdot}574 \ln T - (297{\cdot}75 - 11{\cdot}91\ P)/T. \tag{5.2}$$

Comparison of the expressions (4) and (5.1) yields $C = -1{\cdot}574$, $B = 0$, and thus $\Delta C^\circ_p = -3{\cdot}13$ cal/deg and $\Delta H^\circ = -(3{\cdot}13)\,T$ cal for the exchange equilibrium, a between 975–1400 °C at 25 kb. The ΔC°_p is expected to vary as a function of temperature, so that this value should be taken to represent the average value of ΔC°_p in the temperature range 975–1400 °C.

Figure 4 shows a conventional plot of $\ln K_D$ vs. $1/T$ according to the regressed expressions

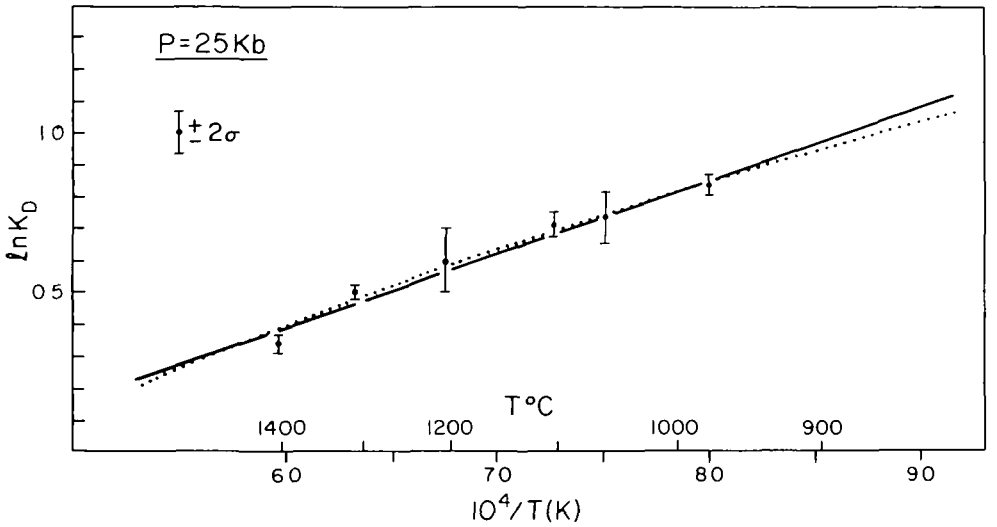

FIG 4. $\ln K_D$ versus reciprocal temperature The data with vertical bars represent mean with 2σ uncertainty of the reversed experimental determinations in the FMAS system. All data are normalized to 25 kb. The solid and dotted lines represent least squared fits to all (23) experimental data according to the assumptions of $\Delta C_p^\circ = 0$ and ΔC_p° = constant, but nonzero, respectively

(3.1) and (5.1), along with the experimental data. There is little difference between the two fits in the temperature range of our experiments, but the extrapolations to around 700 °C (which is an approximate lower limit for application to most natural assemblages) yields temperatures that differ by about 50 °C. We performed an additional experiment at 20 kb, 750 °C with $PbO–PbF_2$ for one week to constrain the low temperature exchange equilibrium. However, it failed to yield any significant reaction between garnet and orthopyroxene even though the flux was molten in the charge.

Figure 5 shows a comparison of our results on the temperature dependence of $\ln K_D$ with the experimental results of Kawasaki & Matsui (1983) and Harley (1984) in the FMAS system. All data are normalized to 25 kb. The various experimental results agree within the limits of their uncertainties. However, the best fit to Harley's data lies about 70–85 °C lower than the linear least squared fit to our data.

Harley (1984) performed some of his experiments in iron capsules, and noted substantial iron addition to the charge from the encapsulating material. He revised the $\ln K_D$ values upward by 0·15–0·20 units on the basis of the observation that the run 'in graphite capsules with mixes not susceptible to Fe-addition' yielded $\ln K_D$ values greater by the above magnitude compared to those made in Fe capsule. The K_D values obtained through these arbitrary adjustments may not be very precise. Further, the data shown in Fig. 2 and those of Kawasaki & Matsui (1983, fig. 4) do not suggest any significant dependence of K_D on Fe/Mg ratio at the temperatures of Harley's experiments.

Newton, Kleppa and coworkers (Charlu *et al.*, 1975; Chatillon–Colinet *et al.*, 1983*a*,*b*; Brousse *et al.*, 1984; Geiger *et al.*, 1987) have measured the heat of formation, ΔH_f°, from oxides of the iron and magnesium end-member components of orthopyroxene and garnet from heat of solution measurements in lead borate and/or alkali borate solvents. The calorimetric temperatures were 970 and 1023 K, respectively. The ΔH_{sol} of iron end-members were measured in alkali borate solution at 1023 K, whereas those for magnesium

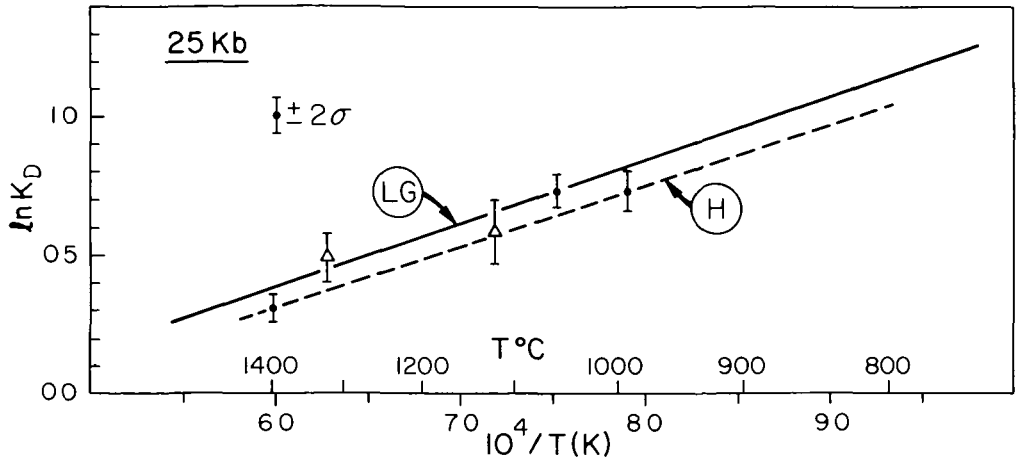

FIG. 5 Comparison of the $\ln K_D$ vs. $1/T$ relation determined in this work (LG: solid line) with the experimental determinations of Kawasaki & Matsui (1983), shown by triangles, and Harley (1983, H: dashed line).

end-members were measured in both lead borate and alkali borate solvents. There are some significant differences in the derived ΔH_f° values depending on the nature of calorimetric solvent; further, for the iron end-members, ΔH_f° was found to depend on whether the ΔH_{sol} of the oxides was based on the dissolution of stoichiometric mixtures of fayalite + quartz, or separate dissolution of fayalite and quartz (Chatillon-Colinet *et al.*, 1983*a*).

Various combinations of the ΔH_f° of the end-member components derived from calorimetric measurements, discussed above, yield a very wide range of values, -2877 (± 742) to -4500 (± 850) cal, for the ΔH° of the Fe–Mg exchange equilibrium *a* at 1 b, 1023 K. This is too wide a range of value for ΔH_a° to impose any significant constraint on the Fe–Mg fractionation between garnet and orthopyroxene. The accrued errors in the calorimetric ΔH_a° values may be reduced by using ΔH_f° values which are derived by following similar procedures. Thus, we adopt only measurements from alkali borate calorimeter, since the necessary complete set of determinations are not available in lead borate solvent. This procedure yields $\Delta H_a^\circ = -3921(\pm 755)$ cal at 1 b, 1023 K, which is in excellent agreement with the value -3916 (± 282) cal derived from experimental determination of Fe–Mg fractionation, if the data are fitted by a linear relation of $\ln K_D$ vs. $1/T$ (eqn. 3.2), and extrapolated to 1023 K. It makes no significant difference whether the dissolution data for fayalite + quartz or separate dissolution data for fayalite and quartz are used to calculate ΔH_f° for almandine and ferrosilite, as long as the same procedure is used for both minerals. The expression (5.2), on the other hand, yields ΔH°(1 b, 1023 K) $= -2607$ (± 183) cal, which agrees only marginally with the values derived from calorimetric measurements. Thus, the linear regression of $\ln K_D$ vs. $1/T$ may be a more appropriate treatment of the experimental data, at least in the range of temperature of geological interest.

Thermodynamic analysis of the effect of Fe/Mg ratio on K_D

There has been considerable progress in recent years in the determination of Fe–Mg mixing properties in garnet and orthopyroxene. Even though these data are not completely adequate to tightly constrain the effect of Fe/Mg ratio on K_D, it is still instructive to

compare the experimentally determined relation between Fe/Mg ratio and K_D with that predicted from the available thermodynamic data.

From analysis of the compositional data of garnet and coexisting silicates in natural assemblages and limited experimental data on Mg-rich composition, Ganguly & Saxena (1984) have predicted that the almandine and pyrope components have an asymmetric positive excess free energy of mixing. Geiger *et al.* (1987) have recently determined ΔH^{mix} of pyrope and almandine by solution calorimetry at 760 °C, which compares well with the ΔG^{xs} predicted by Ganguly & Saxena (1984). This agreement suggests that the excess entropy of mixing, ΔS^{xs}, in the Fe–Mg binary of garnet should be very small. On the basis of calorimetric ΔH^{mix} data and available cation ordering data (Saxena & Ghose, 1971) Chattilon–Colinet *et al.* (1983*b*) have concluded that (Fe, Mg) SiO_3 orthopyroxene behaves 'very nearly ideally' down to at least 700 °C.

Assuming the Fe–Mg join of orthopyroxene to be ideal, and that of garnet to be asymmetric which can be described by Margules relation (see Ganguly & Saxena, 1987),

$$\Delta G^{xs} = (\bar{W}_G^{MgFe} X_{Fe} + \bar{W}_G^{FeMg} X_{Mg}) X_{Fe} X_{Mg},$$

we obtain

$$RT\ln K_\gamma \simeq RT\ln\left(\frac{\gamma_{Fe}}{\gamma_{Mg}}\right)^{Gt} \approx \{\bar{W}_G^{FeMg} X_{Mg}^2 - \bar{W}_G^{MgFe} X_{Fe}^2 + 2X_{Fe} X_{Mg}(\bar{W}_G^{MgFe} - \bar{W}_G^{FeMg})\}^{Gt} \quad (6)$$

According to Ganguly & Saxena (1984), $\bar{W}_G^{FeMg} = 200$ and $\bar{W}_G^{MgFe} = 2500$ cal/cation, whereas Geiger *et al.* (1987) give $\bar{W}_H^{FeMg} = -1256$ and $\bar{W}_H^{MgFe} = 2882$ cal/cation as the best fit to their calorimetric enthalpy of mixing data according to Margules relation (note that $\bar{W}_G = \bar{W}_H - T\bar{W}_S$). Using these values and combining (1) and (6), we have calculated the ratio K_D/K vs. X_{Fe} at several P–T conditions. The results for 1200 °C, 26 kb are compared with the reversed experimental data in Fig. 6. Using the Ganguly–Saxena mixing model (1984) we get $K_D/K = 1$ at $X_{Fe} = 0{\cdot}65$, whereas with the Geiger *et al.* (1987) model (and $W_S = 0$), $K_D/K = 1$ at $X_{Fe} = 0{\cdot}72$.

As evident from Fig. 6, K_D vs. X_{Fe} relations predicted by the above mixing property data do not agree with that determined experimentally. The experimental data suggest that either the Fe–Mg solid solution in garnet becomes nearly ideal at $T \geq 1200$ °C, or that the orthopyroxene solid solution is nonideal at these conditions such that it approximately compensates for the effect of Fe–Mg nonideality in garnet solid solution on K_D.

Effect of alumina solubility in orthopyroxene on K_D

The effect of the variation of Al_2O_3 content in orthopyroxene on K_D will be manifested through that on $(\gamma_{Fe}/\gamma_{Mg})^{OPx}$ (eqn. 1). The importance of this effect may be illustrated by assuming orthopyroxene as a ternary 'Simple Mixture' (see Ganguly & Saxena, 1987) of $FeSiO_3$, $MgSiO_3$, and Al_2O_3 components in FMAS system. We can then write, following Ganguly & Kennedy (1974),

$$RT\ln\left(\frac{\gamma_{Fe}}{\gamma_{Mg}}\right)^{OPx} = W_{FeMg}^{OPx}(X_{Mg} - X_{Fe})^{OPx} + (\Delta W X_{Al_2O_3})^{OPx} \quad (7)$$

where W_{ij}^{OPx} is a 'Simple Mixture' interaction parameter, and $\Delta W = W_{FeAl} - W_{MgAl}$.

Since orthopyroxene behaves very nearly ideally at $T > 700$ °C (Chatillon–Colinet *et al.*, 1983*b*), the first term after equality should be negligible. Also, for the same reason, the ΔW

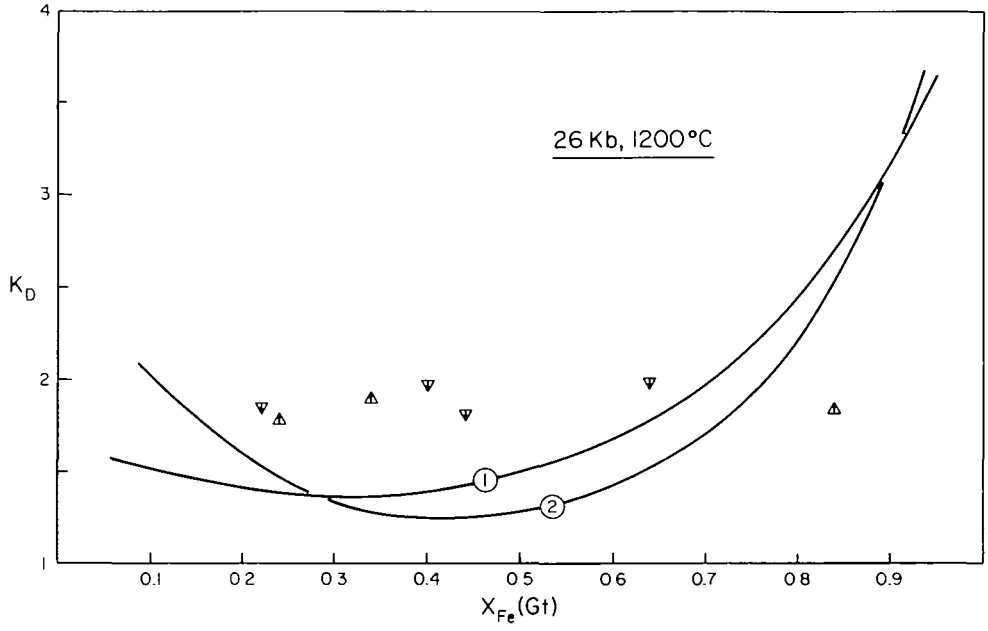

FIG. 6 Comparison of the dependence of K_D on X_{Fe}(Gt) in FMAS system, calculated from the available thermodynamic mixing property data with that determined experimentally at 26 kb, 1200°C The symbols point towads the direction of approach of equilibrium. The orthopyroxene solid solution is assumed to be ideal. The curves 1 and 2 correspond to garnet mixing data according to Ganguly & Saxena (1984) and Geiger *et al.* (1987), respectively.

term should be very small. In our experiments, the Al_2O_3 content of orthopyroxene varied approximately between 1 and 4 mol per cent (Table 2). Consequently, even allowing for a magnitude of 1 kcal for the ΔW term at 1000 °C, 4 mol per cent Al_2O_3 leads to a change of $\ln(\gamma_{Fe}/\gamma_{Mg})^{OPx}$ of 0·016, which corresponds to a change of K_D by a factor of 1·016. Thus, we conclude that the variation of Al_2O_3 solubility in orthopyroxene is of no practical significance in the determination of equilibrium K_D values in the FMAS system.

Alumina solubility in orthopyroxene

We have adequate data to constrain the effect of FeO on Al_2O_3 solubility in orthopyroxene in equilibrium with garnet only at two sets of P–T conditions, 20 kb, 975 °C and 25 kb, 1200°C. These results are illustrated in Fig. 7. Most of these data were obtained from runs made primarily for the determination of Fe–Mg fractionation, in which the starting mixture consisted of *nonaluminous* orthopyroxene and garnet. A limited number of experiments were carried out with aluminous enstatite (6·4 wt. per cent Al_2O_3) plus Fe–Mg garnet as starting mixtures. The experimental data in Fig. 7 are fitted visually using the data for MAS system (Perkins *et al.*, 1981) as constraints and considering the expected thermodynamic form of the fit.

The thermodynamic form of the effect of iron on the alumina solubility in orthopyroxene in equilibrium with garnet may be illustrated by treating the granet–orthopyroxene equilibrium as follows.

$$\underset{\text{OPx}}{3\,MgSiO_3} + \underset{\text{OPx}}{Al_2O_3} = \underset{\text{Gt}}{Mg_3Al_2Si_3O_{12}} \qquad \text{(b)}$$

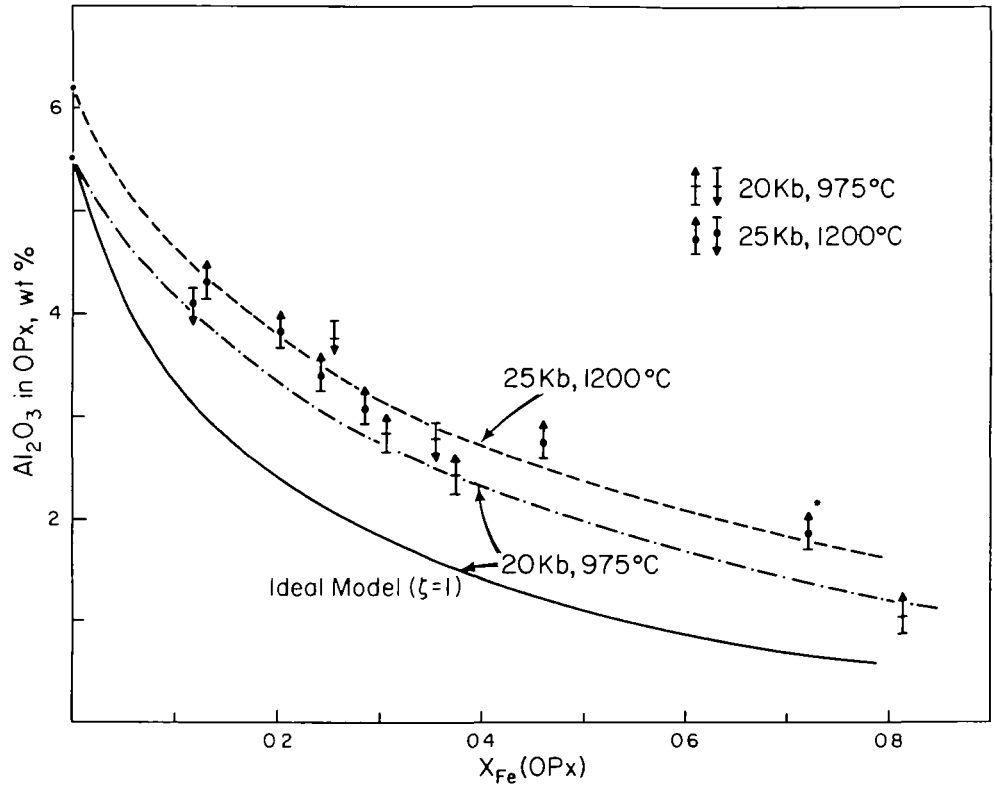

FIG. 7. Experimental data on the alumina solubility in orthopyroxene in equilibrium with garnet in the FMAS system at (a) 20 kb, 975 °C, and (b) 25 kb, 1200 °C. Upward and downward pointing arrows indicate direction of approach to equilibrium. The orthopyroxene starting compositions in the upward pointing arrows were free of alumina, whereas those in the downward pointing arrows were free of iron. The half-length of the arrows represents the 1σ uncertainty of the final compositions. The datum marked with an asterisk was obtained from a run at 30 kb, 1200 °C; the alumina solubility in OPx at 25 kb, 1200 °C should be somewhat higher as the solubility decreases with increasing pressure. The data are fitted visually, considering the expected thermodynamic form of the fit, and using the alumina solubility data in MAS system (Perkins *et al.*, 1981) as constraints.

where Al_2O_3 is a hypothetical component with orthopyroxene structure. At equilibrium

$$K_{(b)} = \left[\frac{(X_{Mg}^{Gt})^3}{(X_{Mg}^{OPx})^3 (X_{Al_2O_3}^{OPx})}\right] K_{\gamma(b)}. \tag{7}$$

Here $X_i^{OPx} = i/(MgSiO_3 + Al_2O_3 + FeSiO_3 + \ldots)$ in OPx and $K_{\gamma(b)}$ collectively denotes the activity coefficient terms in the expression of the equilibrium constant.

From garnet–orthopyroxene equilibrium in the MAS system, we also have

$$K_{(b)} = \left[\frac{1}{(X_{Mg}^{OPx})^3 (X_{Al_2O_3}^{OPx})}\right] K_{\gamma(b)}^{MAS} = (K_X^{MAS})(K_{\gamma(b)}^{MAS}). \tag{8}$$

Equating (7) and (8), and rearranging terms, we get

$$X_{Al_2O_3}^{OPx} = \left(\frac{X_{Mg}^{Gt}}{X_{Mg}^{OPx}}\right)^3 \left(\frac{1}{K_X^{MAS}}\right)\left(\frac{K_{\gamma(b)}}{K_{\gamma(b)}^{MAS}}\right) \tag{9}$$

Note that $K_{\gamma(b)}$ and $K^{MAS}_{\gamma(b)}$ refer to the 'activity coefficient terms' in a general multi-component system and in the MAS system, respectively, and are not necessarily equal. Using the definition of K_D (eqn. 1), the expression (9) can be rewritten as

$$X^{OPx}_{Al_2O_3} = \left[\frac{1}{1+X^{OPx}_{Fe}(K_D-1)}\right]^3 \left[\frac{1}{K^{MAS}_X}\right]\zeta \qquad (10)$$

where ζ stands for the ratios of $K_{\gamma-s}$ in eqn. (9).

At fixed P–T condition, K^{MAS}_X is a constant. Thus, since $K_D > 1$ (Fig. 3), $X_{Al_2O_3}$ is expected to decrease exponentially with X_{Fe}. The special case for $\zeta = 1$ is illustrated in Fig. 7 for P–T condition of 20 kb, 975 °C. It agrees with the experimentally determined relation within 1 wt. per cent Al_2O_3 in orthopyroxene. For 25 kb, 1200 °C, the 'ideal' approximation underestimates alumina solubility in orthopyroxene by less than 0·5 wt. per cent. The choice of $MgAl_2SiO_6$ (Mg-tschermak) or $Mg_3Al_2Si_3O_{12}$ (orthopyrope) as aluminous orthopyroxene components does not seem to improve the agreement between the experimental data and 'ideal' approximation.

Wood (1974), Harley (1984) and Bertrand *et al.* (1986) have derived expressions to describe the effect of FeO on Al_2O_3 solubility in orthopyroxene in equilibrium with garnet. The relations obtained from these expressions at 20 kb, 975 °C and 25 kb, 1200 °C are compared with the visual fits to our experimental data in Fig. 8. Our experimental data suggest stronger effect of FeO on the Al_2O_3 solubility in orthopyroxene in the compositional range of natural garnet-lherzolites.

Figure 9 shows a comparison of the effects of calcium, iron, and chromium concentrations in garnet on the alumina solubility in coexisting orthopyroxene. The data for the effects of calcium (CMAS system) and chromium (MASCr) are from Perkins & Newton (1980) and Chatterjee & Terhart (1985), respectively. All data have been constrained by reversed experiments at selected P–T conditions. The results suggest that the divalent and trivalent cation substitutions in garnet at least up to about 15 mol per cent have similar

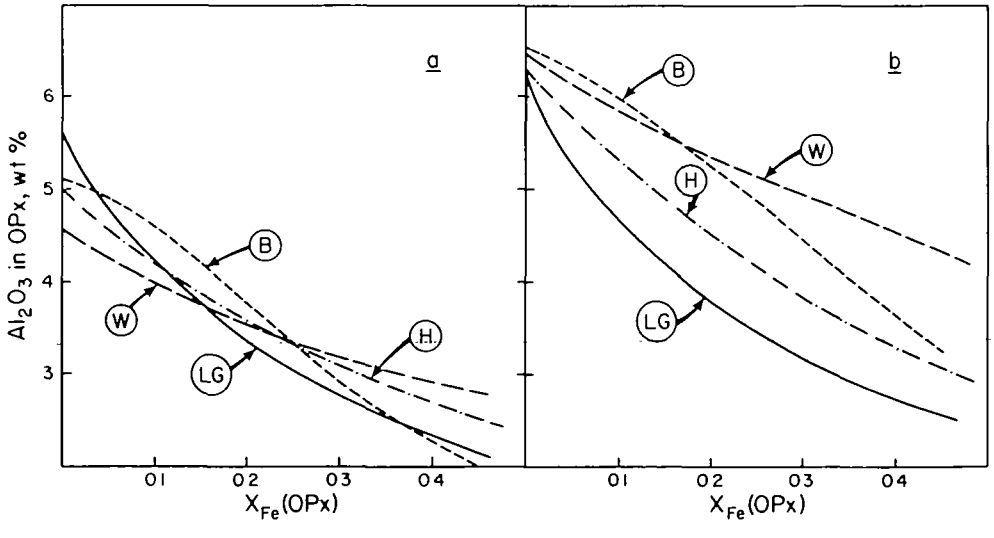

FIG. 8. A comparison of the effect of FeO on alumina solubility, as determined in this study (LG), with those obtained from the relations proposed by Wood (1974: W), Harley (1984: H), and Bertrand *et al.* (1986: B). (a) 20 kb, 975 °C, (b) 25 kb, 1200 °C.

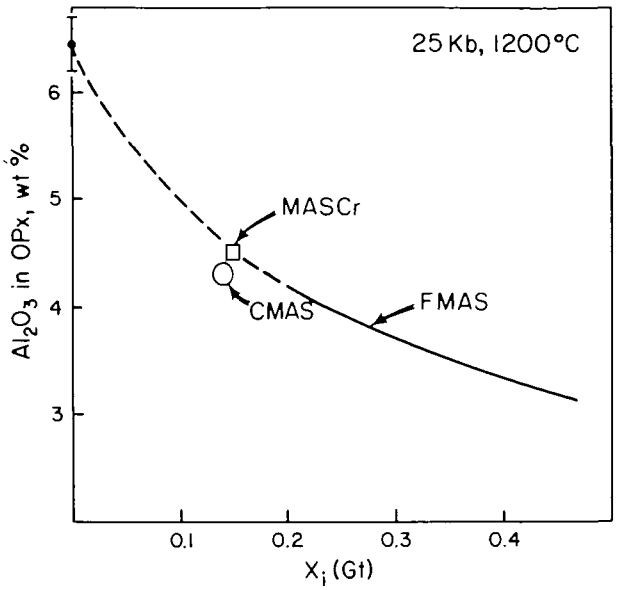

FIG. 9. Comparison of the experimental data on the effect of garnet composition on the alumina solubility in coexisting orthopyroxene at 25 kb, 1200°C. CMAS: Perkins & Newton (1980), MASCr: Chatterjee & Terhart (1986); FMAS: This study. The MAS datum represents the average from Lane & Ganguly (1979), Perkins *et al* (1981), and Chatterjee & Terhart (1986).

effect on the alumina solubility in coexisting orthopyroxene. The effect of simultaneous substitution of the divalent and trivalent cations will be less than the sum of the individual effects owing to reciprocal interaction which contributes to positive deviation from ideality in garnet solid solution (Wood & Nicholls, 1978).

The equilibrium pressures of garnet-lherzolite xenoliths are often estimated on the basis of data on alumina solubility in orthopyroxene in MAS system without correction for the effects of additional components (e.g., Finnerty & Boyd, 1984; Ganguly & Bhattacharya, 1987). Although there are still inadequate experimental and thermodynamic data to make appropriate corrections for the compositional effects, it is clear from Fig. 9 that in natural assemblages, the Al_2O_3 in orthopyroxene in equilibrium with garnet could be significantly lower than that in MAS system at the same $P-T$ condition.

In natural garnet-lherzolites, there is often 25 mol per cent of Ca+Fe in the divalent cation site of garnet, and the Al_2O_3 in coexisting orthopyroxene is around 1 wt. per cent. If we assume that in the natural assemblages the alumina solubility in orthopyroxene is diluted by the addition of Ca+Fe in the same proportion as shown in Fig. 9, then it seems that the pressures of natural assemblages with about 25 mol per cent Ca+Fe had been overestimated by about 5 kb by the direct application of the data for the MAS system.

GARNET–ORTHOPYROXENE GEOTHERMOMETER

The application of the Fe–Mg fractionation data to the geothermometry of natural assemblages obviously require correction for the effects of additional components which can substitute significantly in garnet and orthopyroxene solid solutions. The major substitutional cations in natural assemblages are Ca, Mn, and Cr^{3+}. The last one is usually

unimportant in crustal assemblages, but may have significant effect in mantle xenoliths (Wood & Nicholls, 1978).

Mn and Ca substitute highly preferentially in garnet relative to coexisting orthopyroxene (e.g., Dahl, 1980). Consequently, the effect of possible nonideal interactions of Mn and Ca in orthopyroxene on K_D is usually expected to be negligible compared to those in garnet, especially in the range of compositions of *common* natural assemblages. Thus, following the treatment of Ganguly & Saxena (1984: eqns. 2 and 12) on Fe–Mg exchange geothermometry between garnet and a coexisting phase in the Fe–Mg–Mn–Ca system, and *assuming* K_D *to be independent of Fe/Mg ratio*, we can recast (3.1) and (5.1) into the following geothermometric expressions, respectively.

$$T \approx \frac{1971 + 11{\cdot}91P + \frac{1}{R}(\Delta W_{Ca} X_{Ca} + \Delta W_{Mn} X_{Mn})^{Gt}}{\ln K_D + 0{\cdot}96} \qquad (11.1)$$

and

$$\frac{1}{T}\left[\frac{\Delta W_{Ca}}{R} X_{Ca}^{Gt} + \frac{\Delta W_{Mn}}{R} X_{Mn}^{Gt} - 297{\cdot}75 + 11{\cdot}91P\right] - 1{\cdot}574 \ln T \approx \ln K_D - 12{\cdot}067 \qquad (11.2)$$

where T is in °K and P is in kb.

In view of the calorimetric data discussed earlier, expression (11.1) may be preferable to (11.2), but both need to be tested in future.

According to Ganguly & Saxena (1984), $\Delta W_{Ca} \approx \Delta W_{Mn} \approx 3000$ (± 500) calories per mol of cation for $X_{Ca}^{Gt} \leq 0{\cdot}30$ and $X_{Mn}^{Gt} \leq 0{\cdot}30$. These values may be substituted in (11.1) and (11.2) to obtain explicit solution of temperatures. In order to obtain a numerical solution for T in eqn. (11.2), it is advantageous to use the analytical solution from (11.1) as an initial guess. The equation (11.2) can then be solved for T easily by successive approximations. As evident from Fig. 4, the two equations should yield approximately the same temperature between 950 and 1400°C. At other temperatures, $T(11.2) < T(11.1)$; the approximate difference between the two solutions at various temperatures should be evident from Fig. 4.

The assumption of the independence of K_D on Fe/Mg ratio, which has been used to develop the geothermometric expressions above, is well justified by our experimental data and those of Kawasaki & Matsui (1983) for $T \gtrsim 1000$°C (that is for most assemblages in mantle derived xenoliths), but may not be valid at significantly lower temperature. Thus, the application of the geothermometer to granulite facies assemblages should be made with caution.

We do not, as yet, have adequate mixing property data to correct for the effect of Cr^{3+}. It mixes almost ideally with Al in garnet solid solution (Mattioli & Bishop, 1984; Wood & Kleppa 1984). However, substitution of Cr^{3+} in garnet would still affect K_D owing to the following reciprocal equilibrium in garnet, $Fe_3Cr_2Si_3O_{12} + Mg_3Al_2Si_3O_{12} \leftrightarrows Mg_3Cr_2Si_3O_{12} + Fe_3Al_2Si_3O_{12}$. Assuming ideality of mixing between Cr^{3+} and Al in garnet, the effect of the reciprocal equilibrium on K_D can be expressed as $\partial \ln K_D / \partial X_{Cr}^{Gt} = \Delta G_r^\circ / RT$ (see Wood & Nicholls, 1978; Ganguly & Saxena, 1987), where ΔG_r° is the standard free energy change of the reciprocal reaction. There are no data to constrain ΔG_r°, but the value for the standard free energy change for analogous reciprocal reaction in spinel solid solution (Wood & Nicholls, 1977) suggests that the magnitude of ΔG_r° may be quite significant. Thus, the above expressions may not yield reliable temperature for Cr^{3+} rich compositions.

In common with virtually any other geothermometer (or geobarometer) based on the composition of the coexisting minerals, the major uncertainties in the application of the

above thermometer to natural assemblages are due to those in the mixing property terms and determination of equilibrium compositions by microprobe analyses. It can be shown that a given percentage uncertainty in K_D translates into approximately half of that in the temperature estimate. (This problem is even worse with cation exchange geothermometers such as garnet–biotite which have flatter $\ln K_D$ vs. $1/T$ slopes.) Thus, considering the various factors, we believe that the uncertainties in the mixing property and analytical data will contribute an uncertainty of around 30–50 °C to the temperature estimate of most natural assemblages, at least above 1000 °C, if the equilibrium mineral compositions were determined carefully.

The application of (11.1) to 36 garnet-lherzolite xenoliths from Lesotho, South Africa, yields temperatures that are systematically higher, on the average by 78 °C, compared to the 'mean of 5 preferred methods', and by 58 °C compared to the 'mean of 10 preferred methods' of Carswell & Gibb (1980). The temperature of these garnet-lherzolite nodules fall in the range of 950–1500 °C. There is, however, no objective reason for preferring the 'preferred methods' of Carswell & Gibb (1980) to the expression (11.1).

We have also applied the above geothermometric formulations to a large number of granulite facies assemblages described in the literature (Dahl, 1979; Wells, 1979; Glassley & Sorensen, 1980; Janardhan *et al.*, 1982; and the extensive data set compiled by Perkins &

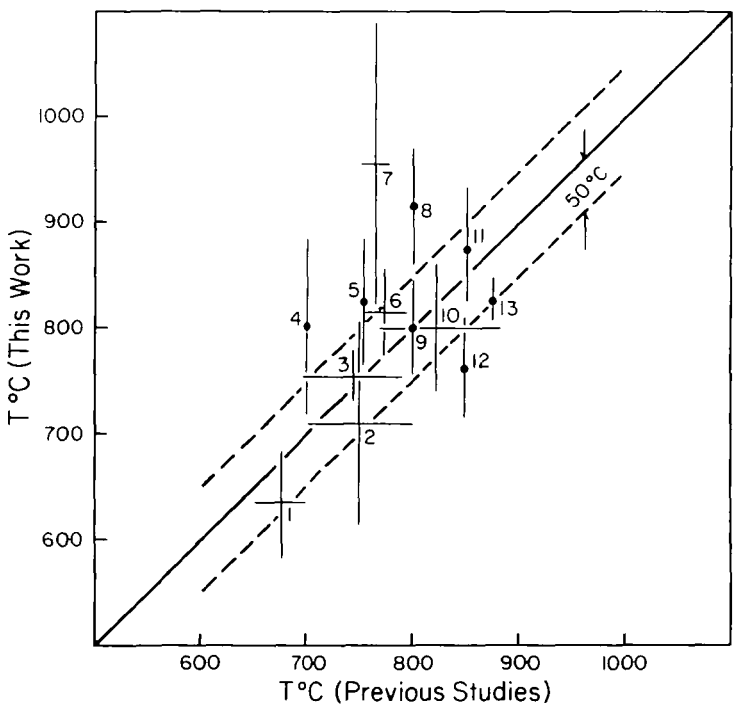

FIG. 10. Comparison of the temperatures of granulite facies assemblages determined from (11.1) with those in the earlier studies. Excepting 3 and 10, Nos. 1 through 12 are calculated using the data compiled by Perkins & Chipera (1985). 1: Granite Falls, Minnesota; 2: English River, Ontario; 3: Kelley Iron Formation, Montana (Dahl, 1979); 4: Otter Lake, Quebec; 5: Inarijarvi Complex, Finland; 6: Nain Province, Labrador; 7: Adirondacks, New York; 8. Furua Complex, Tanzania; 9: Buksfjorden, Greenland; 10: 'Highland' charnockites, India (Janardhan *et al.*, 1982); 11: Qianxi Complex, China; 12: Molodezhnaya Station, Antarctica; 13: Agto, west Greenland (Glassley & Sorenson, 1980). The length of the bars represent the spread of the estimated temperature.

Chipera, 1985). The estimated temperatures, based on expression (11.1), versus the original estimates, are illustrated in Fig. 10. Much of the original estimates are based on geological constraints or geothermometers, which were in fairly initial stages of development, so the extent of their agreement with the present results do not have much implication about the validity of our formulation.

The main implications of Fig. 10 are in suggesting potential problems with certain assemblages, and showing the spread of temperature of granulite facies assemblages. Most of the original estimates, however, agree to within ± 50 °C of the present results. Among those that are in good agreement with our results, the 'highland' charnockite samples from India (Janardhan *et al.*, 1982) and the granulites from Kelley iron formation of Montana (Dahl, 1979) are noteworthy as the original estimates were based, at least in our judgment, on judicious application of the available geothermometers. Of the samples that strongly disagree with our results, the Adirondack samples are particularly noteworthy. The original temperatures were based on two feldspar and/or iron-titanium oxide thermometry on what seems to be carefully selected samples and careful microprobe data (Bohlen & Essene, 1979, 1980). Recalculation (equation 11.1) of the Adirondack samples treating total iron as FeO reduces the mean temperature by ~ 55 °C and the spread to ± 90 °C from ± 135 °C. We are unable to explain the problem with the Adirondack samples, but note that Perkins & Chipera (1985) have also found the most discordant results in the geobarometry of these samples based on their calibration of the complementary equilibria grossular + pyrope + quartz = anorthite + enstatite and grossular + almandine + quartz = anorthite + ferrosilite. They have also found highly discordant results for the Otter Lake samples. There is no obvious systematic compositional dependence of the inferred temperatures of the granulite samples. Further work is needed in the refinement of the geothermometer as well as in the determination of equilibrium compositional data of the discordant natural samples.

ACKNOWLEDGEMENTS

Thanks are due to Dr. Robert C. Newton for discussions about the calorimetric data, and Dr. Michael Drake and Tom Teska for providing the facilities for microprobe analytical techniques. The paper has greatly benefited from thorough and constructive reviews of Drs. Dexter Perkins, David Pattison, Eric Essene and Lawrence Anovitz. The senior author is also grateful to Drs. Paul Damon, Christopher Eastoe, and Joaquin Ruiz for their interest in this work and helpful suggestions during the course of his Ph.D. dissertation, which formed the basis of this paper. The research was supported by a grant from U.S. National Science Foundation, No. EAR-8206656. We are also grateful to Smithsonian Institution for the supply of garnet sample (Collection No. 143895) which was used in the starting mixture.

REFERENCES

Akella, J., & Boyd, F. R., 1973. Effect of pressure on the composition of coexisting pyroxene and garnet in the system $CaSiO_3$–$MgSiO_3$–$FeSiO_3$–$CaAlTi_2O_6$. *Yb. Carnegie Inst. Wash.* **72**, 523–26.

—— Ganguly, J., Grover, R., & Kennedy, G. C., 1972. Melting of lead and zinc to 60 kb. *J. Phys. Chem. Solids* **34**, 631–36.

Bence, A. E., & Albee, A. L., 1968. Empirical correction factors for the electron microanalysis of silicate and oxides. *J. Geol.* **76**, 382–403.

Bertrand, P., Sotin, C., Mercier, J. C. C., & Takahashi, E., 1986. From the simplest chemical system to the natural one: garnet peridotite barometry. *Contr. Miner. Petrol.* **93**, 168–78.

Boettcher, A. L., Windom, K. E., Bohlen, S. R., & Luth, R. W., 1981. Low-friction anhydrous low- to high-temperature furnace assembly for piston-cylinder apparatus. *Rev. Sci. Instrum.*, **52**, 1903–4.

Bohlen, S. R., & Essene, E. J., 1979. Critical evaluation of two-proxene thermometry in Adirondack granulites. *Lithos*, **12**, 335–45.

——— 1980. Evaluation of coexisting garnet-biotite, garnet-clinopyroxene, and other Mg-Fe exchange thermometers in Adirondack granulites. *Geol Soc. Am. Bull* **91**, Part 1, 685–719

Brousse, C., Newton, R. C., & Kleppa, O. J., 1984. Enthalpy of formation of forsterite, enstatite, akermanite, monticellite and merwinite at 1073 K determined by alkali borate solution calorimetry. *Geochim. cosmochim Acta*, **48**, 1081–8

Carswell, D. A., & Gibb, G. F, 1980. Geothermometry of garnet lherzolite nodules with special reference to those from the kimberlites of Northern Lesotho. *Contr. Miner. Petrol.* **74**, 403–16.

Charlu, T. V., Newton, R. C., & Kleppa, O. J., 1975. Enthalpies of formation at 970K of compounds in the system $MgO–Al_2O_3–SiO_2$ from high temperature solution calorimetry. *Geochim. cosmochim. Acta*, **39**, 1487–97.

Chatillon-Colinet, C., Kleppa, O. J., Newton, R. C., & Perkins, D., 1983*a*. Enthalpy of formation of $Fe_3Al_2Si_3O_{12}$ (almandine) by high temperature alkali borate solution calorimetry. *Ibid.* **47**, 439–44

—— Newton, R. C., Perkins, D., & Kleppa, O. J., 1983b. Thermochemistry of $(Fe^{2+}, Mg)SiO_3$ orthopyroxene. *Ibid* **47**, 1597–603

Chatterjee, N, 1987. Evaluation of thermochemical data on Fe–Mg olivine, orthopyroxene, spinel and Ca–Fe–Mg garnet. *Geochim. cosmochim. Acta*, **51**, 2515–26

Chatterjee, N D., & Terhart, L., 1985. Thermodynamic calculation of peridotite phase relations in the system $MgO–Al_2O_3–SiO_2–Cr_2O_3$, with some geological applications. *Contr. Miner. Petrol.* **89**, 273–84.

Dahl, P. S., 1979. Comparative geothermometry based on major element and oxygen isotope distributions in Precambrian metamorphic rocks from southwest Montana. *Am. Miner.* **64**, 1280–94.

—— 1980. The thermal-compositional dependence of Fe–Mg distributions between coexisting garnet and pyroxene. Application to geothermometry. *Ibid.* **65**, 854–66.

Elphick, S C., Ganguly, J., & Loomis, T. P., 1985. Experimental determination of cation diffusivities in aluminosilicate garnets. I. Experimental methods and interdiffusion data. *Contr. Miner. Petrol.* **90**, 36–44.

Finnerty, A. A., & Boyd., 1984. Evaluation of thermobarometer for garnet peridotites. *Geochim. cosmochim. Acta*, **48**, 15–27

Ganguly, J., Bhattacharya, P K., 1987. Xenolith in Proterozoic kimberlites from southern India. Petrology and geophysical implications. In: Nixon, P. H. (ed.) *Mantle Xenoliths*. New York: John Wiley & Sons, 249–65.

—— Bhattacharya, R. N., & Chakraborty, S., 1988. Convolution effect in the determination of compositional profiles and diffusion coefficients by microprobe spot analysis. Am. Miner. in press.

—— Saxena, S. K., 1984. Mixing properties of aluminosilicate garnets. constraints from natural and experimental data, and applications to geothermo-barometry. Am. Miner. **69**, 88–97.

——— 1987. *Mixtures and Mineral Reactions*. New York, Berlin, Heidelberg: Springer-Verlag.

Gasparik, T, 1983. Pyroxene–garnet–corundum equilibria in the system $CaO–MgO–Al_2O_3–SiO_2$. *EOS, Trans. Am. Geophys. Union*, **64**, 347.

—— Newton, R. C., 1984. The reversed alumina contents of orthopyroxene in equilibrium with spinel and forsterite in the system $MgO–Al_2O_3SiO_2$. *Contr. Miner. Petrol.* **85**, 186–96.

Geiger, C. A., Newton, R. C., & Kleppa, O. J., 1987. Enthalpy of mixing of synthetic almandine-grossular and almandine-pyrope garnets from high temperature solution calorimetry. *Geochim. cosmochim. Acta*, **55**, 1755–63.

Glassley, W. E., & Sorenson, K., 1980. Constant *P–T* amphibolite to granulite facies transition in Agto (West Greenland) metadolerites: Implications and applications. *J. Petrology*, **21**, 69–105.

Harley, S. L., 1984 An experimental study of the partitioning of Fe and Mg between garnet and orthopyroxene. *Contr. Miner. Petrol.* **86**, 359–73.

—— Green, D. H., 1982. Garnet–orthopyroxene barometry for granulites and garnet peridotites. *Nature*, **300**, 697–700.

Hensen, B J., 1973. Pyroxenes and garnets as geothermometers and barometers Yb. Carnegie Inst. Wash. **72**, 527–34.

Janardhan, A. S., Newton, R.C., & Hensen, E. C., 1982. The transformation of amphibolite facies gneiss to charnockite in southern Karnataka and northern Tamil Nadu, India. *Contr. Miner. Petrol.* **79**, 130–49.

Kawasaki, T., & Matsui, Y., 1977. Partitioning of Fe and Mg between olivine and garnet. *Earth planet. Sci. Lett.* **37**, 159–66.

——— 1983. Thermodynamic analyses of equilibria involving olivine, orthopyroxene and garnet. *Geochim. Cosmochim. Acta*, **47**, 1661–79.

Lane, D. L., & Ganguly, J., 1980. Al_2O_3 solubility in orthopyroxene in the system $MgO–Al_2O_3–SiO_2$: A re-evaluation, and mantle geotherm. *J. geophys* Res. **85**, 6963–72.

Levin, E. M., Robbins, C. R., & McMurdie, H. F., 1964. *Phase Diagrams for Ceramists*, vol. 1. Ohio: Amer. Ceram. Society, Inc.

Mattioli, G. S., & Bishop, F. C., 1984. Experimental determination of the chromium-aluminum mixing parameter in garnet. *Contr. Miner. Petrol.* **46**, 1367–72.

McCarthy, J., 1975. Wave dispersive spectrometer and stage automation program. NS-892, Tracor-Northern, Inc., Middleton, WI.

Mirwald, P. W., Getting, I. C., & Kennedy, G. C., 1975. Low friction cell for piston-cylinder high pressure apparatus. *J. geophys. Res.* **80**, 1519–25.

Perkins, D., & Chipera, S. J., 1985. Garnet-orthopyroxene-plagioclase-quartz barometry: Refinement and the application to the English River subprovince and the Minnesota River valley. *Contr. Miner Petrol.* **89,** 69–80.

—— Holland, T. J. B., & Newton, R. C., 1981. The Al_2O_3 contents of enstatite in equilibrium with garnet in the system MgO–Al_2O_3–SiO_2 at 15–40 kb and 900–1600 °C. *Ibid.* **78,** 99–109.

—— Newton, R. C., 1980. The compositions of coexisting pyroxene and garnet in the system CaO–MgO–Al_2O_3–SiO_2 at 900–1100 °C and high pressures. *Ibid.* **75,** 291–300.

Ramberg, H., & DeVore, G.W., 1951. The distribution of Fe^{2+} and Mg^{2+} in coexisting olivines and pyroxenes. *J. Geol.* **59,** 193–210.

Saxena, S. K., & Ghose, S., 1971. Mg^{2+}–Fe^{2+} order–disorder and the thermodynamics of the orthopyroxene crystalline solution. Am. Miner. **56,** 532–59.

Sen, S. K., & Bhattacharya, A., 1984. An orthopyroxene-garnet thermometer and its application to the Madras charnockites. *Contr. Miner. Petrol* **88,** 64–71.

Wells, P. R. A., 1979. Chemical and thermal evolution of Archean sialic crust, southern west Greeland. *J. Petrology*, **20,** 187–226.

Wood, B. J., 1974. The solubility of alumina in orthopyroxene coexisting with garnet. *Contr. Miner. Petrol.* **46,** 1–15.

—— Kleppa, O. J., 1984. Chromium-aluminum mixing in garnet: A thermochemical study. *Geochim. Cosmochim. Acta*, **48,** 1373–77.

—— Nicholls, J., 1978. The thermodynamic properties of reciprocal solid solutions. *Contr. Miner. Petrol.* **66,** 389–400

SYMBOLS AND ABBREVIATIONS

Gt:	Garnet
MgTs:	Magnesium Tschermak, $MgAl_2SiO_6$
OPx:	Orthopyroxene
OPy:	Orthopyrope, a component of pyrope stoichiometry ($Mg_3Al_2Si_3O_{12}$) and orthopyroxene structure
QFM:	Quartz–fayalite–magnetite buffer
WI:	Wustite–iron buffer
WM:	Wustite–magnetite buffer
ΔC_p°:	Isobaric heat capacity change of a reaction when all components are in their pure states
ΔG^{xs}:	Excess Gibbs free energy of mixing
ΔH^{mix}:	Enthalpy of mixing
ΔH_f:	Enthalpy of formation from oxides
ΔH_{sol}:	Enthalpy of solution
ΔH_a°:	Enthalpy change of the reaction (a) when all components are in their respective pure states at 1 bar, T.
$K_{(a)}$:	Equilibrium constant of reaction (a)
K_D:	$(Fe/Mg)^{Gt}/(Fe/Mg)^{OPx}$
P:	Pressure in kilobars
T:	Temperature in degree Kelvin
V°:	Molar volume of an end-member component
$\bar{W}_G$, $\bar{W}_H$, $\bar{W}_S$:	Margules parameter corresponding to excess free energy, enthalpy and entropy-of-mixing, respectively.
γ_i:	Activity coefficient of the component i involving one mole of exchangeable cation
$(\pm\sigma)$:	Plus and minus one standard deviation
r:	Statistical correlation coefficient
ΔW_i	$(W_{Mg-i} - W_{Fe-i})$ where the Ws are 'simple mixture' interaction parameters between the specified components in garnet solid solution